J. Membrane Biol. 74, 139–153 (1983)

The Journal of
Membrane Biology

Electrical and Biochemical Properties of an Enzyme Model of the Sodium Pump

J. Brian Chapman, Edward A. Johnson and J. Mailen Kootsey
Departments of Physiology, Monash University, Clayton, Victoria 3168, Australia and
Duke University Medical Center, Durham, North Carolina 27710

Summary. The electrochemical properties of a widely accepted six-step reaction scheme for the Na^+,K^+-ATPase have been studied by computer simulation. Rate coefficients were chosen to fit the nonvectorial biochemical data for the isolated enzyme and a current-voltage (I–V) relation consistent with physiological observations was obtained with voltage dependence restricted to one (but not both) of the two translocational steps. The vectorial properties resulting from these choices were consistent with physiological activation of the electrogenic sodium pump by intracellular and extracellular sodium (Na^+) and potassium (K^+) ions. The model exhibited K^+/K^+ exchange but little Na^+/Na^+ exchange unless the energy available from the splitting of adenosine triphosphate (ATP) was reduced, mimicking the behavior seen in squid giant axon. The vectorial ionic activation curves were voltage dependent, resulting in large shifts in apparent K_m's with depolarization. At potentials more negative than the equilibrium or reversal potential transport was greatly diminished unless the free energy of ATP splitting was reduced. While the pump reversal potential is at least 100 mV hyperpolarized relative to the resting potential of most cells, the voltage-dependent distribution of intermediate forms of the enzyme allows the possibility of considerable slope conductance of the pump I–V relation in the physiological range of membrane potentials. Some of the vectorial properties of an electrogenic sodium pump appear to be inescapable consequences of the nonvectorial properties of the isolated enzyme. Future application of this approach should allow rigorous quantitative testing of interpretative ideas concerning the mechanism and stoichiometry of the sodium pump.

Key Words Na^+,K^+-ATPase · sodium pump · electrogenic · computer simulation · enzyme kinetics · thermodynamics

Introduction

In tissues where a large fraction of time is spent generating action potentials, the net instantaneous active and passive ion fluxes during these action potentials must be comparable in magnitude (Chapman, Kootsey & Johnson, 1979). Although there have been some attempts to explore theoretically the physiological consequences of electrogenic Na^+/K^+ transport in such circumstances, the transport models that were used incorporated purely arbitrary functions to account for the experimentally observed voltage and chemical dependency of the overall transport reaction. Linear dependence on one or more chemical components has been assumed either on the basis of experimental data of limited range (Attwell, Cohen & Eisner, 1979; Brown, Di Francesco, Noble & Noble, 1980; Jakobsson, 1980) or on the basis of the assumptions of irreversible thermodynamics (Rapoport, 1970; Chapman, 1980). Scriven (1981) made the ionic dependences nonlinear in accordance with experimental observation. Chapman et al. (1979) and Johnson, Chapman and Kootsey (1980) treated the pump as an 'elementary-complex' reaction (Keizer, 1975). They also included nonlinear ionic dependences, but constrained them thermodynamically and included the voltage dependence required by thermodynamics.

It is clear that electrogenic Na^+/K^+ transport plays an important role in the electrophysiology of muscle and nerve cells. If that role is to be properly understood, a more accurate description of the transport process is necessary – preferably, one based on a knowledge of the actual mechanism rather than empirical fits or unrealistic treatment as an 'elementary-complex' reaction. Biochemical knowledge of the details of the reaction mechanism underlying Na^+/K^+ transport is sufficiently far advanced to begin to treat the process more realistically as a multi-step enzyme reaction. Biochemical studies give information concerning the number and chemical nature of the individual steps in the transport reaction and the value or approximate magnitude of the rate constants governing these steps.

An enzyme that catalyzes an electrogenic vectorial reaction across a membrane differs from other enzymes in that the equilibrium constant of the overall process depends on the transmembrane potential as well as on the chemical constituents.

This means that the rate coefficients of at least one of the individual elementary steps in the process must be voltage-dependent. Moreover, most transport processes in membranes perform chemical work in addition to electrical work since the activities of the transported species usually differ on the two sides of the membrane. Should, then, the kinetic properties of transport enzymes in their physiological location differ significantly from those manifested by enzymes in solution?

The present paper attempts to explore this general question by examining the physiological behavior of a kinetic model of the electrogenic sodium pump in relation to the biochemical properties of the plasmalemmal Na^+,K^+-ATPase in isolation. Computer simulations of a six-step sequential reaction mechanism adapted from a widely accepted scheme summarized by Guidotti (1979) have been directed to answering questions such as the following:

1. Do the magnitudes and ionic dependences of the active ion fluxes required for physiological function accord with the turnover rates and ionic dependences of the isolated Na^+,K^+-ATPase?

2. Is there a clear relation between the concept of enzyme saturation and the saturation of physiological transport rates as influenced by voltage or ionic composition?

3. Can the unidirectional flux of sodium (Na^+) or potassium (K^+) ions provide a reliable measure of the rate and stoichiometry of net Na^+ or K^+ transport?

4. Does metabolic blockade of the energy supply, as distinct from specific inhibition of the transport ATPase, provide a reliable pharmacological tool for determination of physiological rates of active transport?

These are the kinds of questions that the present paper attempts to address using enzymological modelling methods that extend the approaches already begun independently by Slayman and his coworkers (Gradmann, Hansen & Slayman, 1981; Hansen, Gradmann & Slayman, 1981) and by Chapman (1982). It is not our purpose in the present paper to arrive at a definitive set of states or rate constants, but only to address general questions that do not depend on details of the reaction scheme as yet in question.

The Model

The Sequence of Reactions

The six-step sequential reaction mechanism shown in Fig. 1 is a vectorial adaptation of the scheme

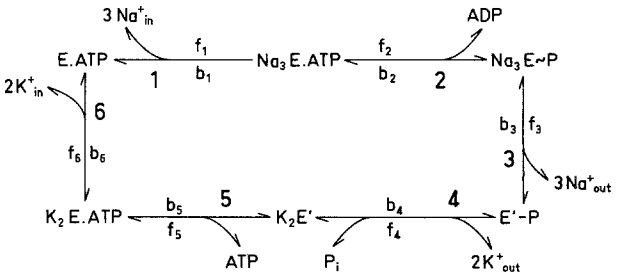

Fig. 1. Reaction scheme for the vectorial Na^+,K^+-ATPase of the electrogenic sodium pump adapted from the mechanism summarized by Guidotti (1979). E and E′ refer to conformationally (translocationally) distinct forms of the enzyme, P_i = inorganic phosphate, ATP and ADP are adenosine tri- and di-phosphate respectively; Na^+_{in}, Na^+_{out}, K^+_{in}, K^+_{out} refer to intracellular and extracellular Na^+ and K^+, respectively; f_i, b_i are the forward and reverse rate coefficients for the i^{th} step

published in Fig. 7 of Guidotti (1979). The intracellular and extracellular forms of Na^+ and K^+ ions are explicitly identified as Na^+_{in}, Na^+_{out}, etc., and the model is simplified to neglect reaction between free enzyme, ATP and Na^+_{in}. This would seem to be reasonable since physiologically the enzyme is surrounded by sufficient reactants and products to reduce the quantity of free enzyme to negligible proportions. As will become apparent later, this simplifying assumption bears little, if any, relation to the "saturation" of the enzyme with respect to physiological transport rates.

Thus, the scheme may be regarded as commencing by reaction between Na^+_{in} and enzyme with ATP already bound (step 1), followed by release of ADP (step 2). Extrusion of Na^+ ions is completed by a conformational change (translocation) and dissociation of the resulting complex (step 3). The enzyme is then dephosphorylated by reaction with K^+_{out} (step 4), followed by a further translocation in which the enzyme binds ATP (step 5). Uptake of K^+ is completed by dissociation of the resulting complex (step 6) which restores the original form of the enzyme capable of reacting with Na^+_{in} at step 1.

We have deliberately refrained from assigning any electric charge to the enzyme intermediates shown in Fig. 1. The charge carried by any intermediate is only relevant in the present context where a step involves movement through an electric field, and its implicit charge value will depend on the kinetic assumptions made in the treatment of voltage dependence (*see below*).

Substrate Competition

It is worth commenting at this stage on the kinds of competition that can occur between the reac-

tants in the scheme of Fig. 1. It can be seen that Na^+_{in} and K^+_{in} compete for one form of the enzyme ($E \cdot ATP$), and Na^+_{out} and K^+_{out} compete for another form ($E'-P$). In each case, however, the consequences of the competition depend on whether Na^+ or K^+ succeeds in reacting with the enzyme. For example, if Na^+_{out} reacts with $E'-P$, the reaction proceeds backwards through step 3 whereas if K^+_{out} reacts then the reaction proceeds forwards through step 4. There is no possibility admitted in this scheme for the kind of competition where *either* Na^+_{out} or K^+_{out} can react backwards in step 3 or forwards in step 4. That is to say, for example, only K^+_{out} can dephosphorylate the enzyme. Although no form of the enzyme can display simultaneous reactivity towards Na^+_{in} and K^+_{out}, or to Na^+_{out} and K^+_{in}, a kind of competition between intracellular and extracellular ions can occur because the total amount of enzyme available is limited. An extracellular ion present in large quantities can commandeer the enzyme in such a way as to reduce ("inhibit") the rates of other steps requiring reaction between intracellular ions and other forms of the enzyme. In this manner, it is theoretically possible for "competitive inhibitory" behavior to be exhibited by all of the reactants in the scheme of Fig. 1. The simulations will show that whether or not such behavior is manifest for any particular reactant depends upon the choice of rate coefficients for the individual steps and upon the free energy available from ATP splitting.

Voltage Dependence

Because the Na^+,K^+-ATPase transport mechanism is electrogenic, one or more of the elementary steps in the overall reaction process must be voltage-dependent. In the absence of experimental evidence the number and location of the voltage-dependent steps must be decided arbitrarily. It seems reasonable to presume that the voltage dependence occurs at one or both of the translocational steps (i.e., steps 3 and 5) since it is there that movement of charge may occur. Three possibilities will be explored:

1. translocation of a trivalent intermediate at step 3 followed by return translocation of a divalent intermediate at step 5.
2. translocation of a univalent intermediate at step 3.
3. translocation of a univalent intermediate at step 5.

The first possibility is conceptually straightforward and involves the assumption that the 3 Na^+ ions and 2 K^+ ions undergo their respective translocations unbalanced by any neutralizing charges.

For the second possibility the 3 Na^+ ions could be translocated by symport with two negative ions, these being returned electroneutrally in association with K^+ ion translocation at step 5. Symport of anions might be achieved by translocation, across the voltage gradient, of negatively charged binding sites on the enzyme.

Similarly, the third possibility could arise from electroneutral translocation of 3 Na^+ ions at step 3 by symport with three balancing charges, these charges being returned in association with K^+ ion translocation at step 5, making step 5 equivalent to the extrusion of one unbalanced positive charge.

For reasons clarified in the results illustrated in Fig. 3 we are inclined to exclude the first as a realistic possibility. Of the remaining two we have chosen the translocation of a univalent charge at step 5. This choice relates to the history of our heuristic approach rather than to any requirement from experimental data.

In either case, the question arises as to the manner in which voltage influences the unidirectional rate coefficients of the elementary reaction step. The fundamental law governing charge transfer reactions is expressed through the Butler-Volmer electrodic equation for a one-step, single charge transfer reaction. This equation may be arranged into a direct, physically representational form given by:

$$i = k_f \cdot a_{in} \cdot \exp((1-\beta)FV/RT)$$

$$-k_b \cdot a_{out} \cdot \exp(-\beta FV/RT)$$

where i is the current carried by the elementary process $A^+_{in} \rightleftharpoons A^+_{out}$, k_f and k_b are its forward and reverse rate coefficients, a_{in} and a_{out} are the respective chemical activities of A^+_{in} and A^+_{out}, V is the electric potential difference between state A^+_{in} and state A^+_{out}, $(V_{in}-V_{out})$; F, R and T have their usual meanings, and β is the so-called symmetry factor (*cf.* Bockris & Reddy, 1970).

The factor β arises from the fact that the electric field modifies an already existent potential energy barrier – the activation energy of the elementary chemical reaction causing the charge movement – thereby imparting voltage dependence to both forward and reverse unidirectional reaction rates. The modification is such that only a fraction $(1-\beta)$ of the input electrical energy appears as a change in activation energy for the forward reaction and, hence, in the forward rate expression;

the remainder (β) appears in the reverse rate expression. This is in contrast to the situation in a semi-conductor junction where, in the absence of an electric field, there is no energy barrier to the movements of electrons/holes. In the presence of an electric field, the energy barrier appears as a 'cliff' with all of the potential energy difference influencing the movement in one direction and none in the other.

In earlier publications where we modelled the electrogenic Na^+/K^+ pump as an 'elementary-complex' reaction (Keizer, 1975) we were forced to treat the voltage dependence in terms of such an energy 'cliff,' with all of the voltage control on the reverse rate of reaction. This restriction of voltage dependence to the reverse rate was necessary in order to obtain a current-voltage relation consistent with the available evidence that the pump acts as a constant-current source in the physiological range (approximately -100 to $+50$ mV) of membrane potentials (Chapman et al., 1979; Johnson et al., 1980; Kootsey, Johnson & Chapman, 1981).

In the absence of any experimental evidence to the contrary, we shall assume a value of 0.5 for the symmetry factor. In the field of electrode reactions where the Butler-Volmer equation was formulated, the experimentally determined values for β are close to 0.5. Indeed, any substantial deviation of β from a value of 0.5 for a supposed elementary step should best be interpreted as suggesting that the process is in fact complex, in which case the apparent value for the symmetry factor may be expected to be significantly voltage-dependent (Fried, 1973).

Materials and Methods

Constraints on Initial Choice of Parameters and Rate Coefficients

The Table lists the normal physiological parameters used as a starting point for exploring the kinetic behavior of the scheme of Fig. 1. Values for the electrochemical boundary conditions were chosen appropriate to cardiac muscle, including the pump site density per unit area of membrane (Michael, Schwartz & Wallick, 1979; Daut & Rudel, 1981). The high energy phosphate levels were deduced from Hassinen and Hiltunen (1975).

The choices of unidirectional rate coefficients for the six elementary steps of the scheme of Fig. 1 were constrained by the following considerations:

1. The ionic activation curves for the nonvectorial ATPase activity had to agree in general shape with those reported by Skou (1957, 1975) for the enzyme isolated from crab nerve.

2. The maximum molecular turnover rate of the enzyme in the nonvectorial situation was not to exceed 10,000 sec^{-1} (167 sec^{-1}) (Jorgensen, 1980).

Table

Parameter	Value	Units
total [ATPase]	$1{\cdot}25\times10^{-13}$	mol/cm^2
$[Na^+]_{in}$	9·6	mmol/liter
$[Na^+]_{out}$	140	mmol/liter
$[K^+]_{in}$	150·4	mmol/liter
$[K^+]_{out}$	5·4	mmol/liter
[ATP]	4·99	mmol/liter
$[P_i]$	4·95	mmol/liter
[ADP]	0·06	mmol/liter
temperature	310	K
f_1	$2{\cdot}5\times10^{11}$	$liter^3mol^{-3}sec^{-1}$
b_1	10^5	sec^{-1}
f_2	10^4	sec^{-1}
b_2	10^5	$liter\,mol^{-1}sec^{-1}$
f_3	172	sec^{-1}
b_3	$1{\cdot}72\times10^4$	$liter^3mol^{-3}sec^{-1}$
f_4	$1{\cdot}5\times10^7$	$liter^2mol^{-2}sec^{-1}$
b_4	2×10^5	$liter\,mol^{-1}sec^{-1}$
f_5	2×10^6	$liter\,mol^{-1}sec^{-1}$
b_5	30	sec^{-1}
f_6	$1{\cdot}15\times10^4$	sec^{-1}
b_6	6×10^8	$liter^2mol^{-2}sec^{-1}$

3. The pseudo first-order rate coefficients for conformational changes (i.e., translocational steps) or for steps involving group transfer by covalent bonds were not to exceed 10^4 sec^{-1}, and the pseudo second-order rate coefficients for diffusion-limited binding steps were not to exceed 10^8 $liter\cdot mol^{-1}s^{-1}$ (Hammes & Schimmel, 1970; Reynolds & Tanford, *personal communication*).

4. The equilibrium constant for the overall pump reaction (equivalent to the product of all forward rate coefficients divided by the product of all reverse rate coefficients) was fixed at 238,722 mol/liter equivalent to a standard free energy of ATP splitting of -31.9 kJ/mol (Hassinen & Hiltunen, 1975; Veech et al., 1979).

5. The resting electrogenic pump current, corresponding to the condition in a quiescent cardiac muscle cell had to be of the order of 0.1 to 0.2 $\mu A/cm^2$ which, with electrical activity, could rise to values of the order of 1 $\mu A/cm^2$ (Johnson et al., 1980). The resting pump current is determined quite rigorously by the fact that the membrane resistance of cardiac muscle is 20 $k\Omega cm^2$ (Mobley & Page, 1972; Lieberman et al., 1975) corresponding to a membrane conductance of 0.05 mS/cm^2. If 80% of this conductance is attributable to potassium ions (i.e., the resting K^+ conductance is 0.04 mS/cm^2) and the Nernst potential for K^+ ions is 5 to 10 mV hyperpolarized relative to the resting potential, then the resting potassium current will be 0.2 to 0.4 $\mu A/cm^2$. In an electrochemical steady state under these conditions it follows that the resting pump current is 0.1 to 0.2 $\mu A/cm^2$ with the passive Na^+, passive K^+ and active pump currents being stoichiometrically determined in the ratio $-3:2:1$ (Chapman et al., 1979).

6. The slope conductance of the pump current-voltage (I–V) relation had to be small in the physiological range of membrane potentials consistent with the common view that the electrogenic pump operates approximately as a constant current source in the physiological range (*cf.* Chapman & Johnson, 1978; Chapman et al., 1979).

Reaction Rate Laws

The following mass action rate laws were used for each of the six elementary steps of the scheme of Fig. 1:

$$rf_1 = f_1[\mathrm{E}\cdot\mathrm{ATP}]\cdot[\mathrm{Na}^+]_{in}^3$$
$$rb_1 = b_1[\mathrm{Na_3E}\cdot\mathrm{ATP}]$$
$$rf_2 = f_2[\mathrm{Na_3E}\cdot\mathrm{ATP}]$$
$$rb_2 = b_2[\mathrm{Na_3E}\sim\mathrm{P}]\cdot[\mathrm{ADP}]$$
$$rf_3 = f_3[\mathrm{Na_3E}\sim\mathrm{P}]$$
$$rb_3 = b_3[\mathrm{E}'-\mathrm{P}]\cdot[\mathrm{Na}^+]_{out}^3$$
$$rf_4 = f_4[\mathrm{E}'-\mathrm{P}]\cdot[\mathrm{K}^+]_{out}^2$$
$$rb_4 = b_4[\mathrm{K_2E}']\cdot[\mathrm{P_i}]$$
$$rf_5 = f_5[\mathrm{K_2E}']\cdot[\mathrm{ATP}]$$
$$rb_5 = b_5[\mathrm{K_2E}\cdot\mathrm{ATP}]$$
$$rf_6 = f_6[\mathrm{K_2E}\cdot\mathrm{ATP}]$$
$$rb_6 = b_6[\mathrm{E}\cdot\mathrm{ATP}]\cdot[\mathrm{K}^+]_{in}^2$$

where rf_i, rb_i are the forward and reverse rates and f_i, b_i are the forward and reverse rate coefficients of the i^{th} step.

The dimensions of the rate coefficients listed in the Table are those appropriate to yield rates of reaction in mol/cm^2/sec. Given that each mole of overall reaction extrudes one Faraday of charge, transport rates in the vectorial situation are expressed as pump current per unit area of membrane. In order to allow a direct quantitative comparison of nonvectorial with vectorial results we have expressed all fluxes (unidirectional or net), transport rates and ATPase activity in the same electrical units. Net ATPase activity is related to the electrical units by noting that pump current (A/cm^2) is given by the pump site density (mol/cm^2) times the Faraday equivalent times the number of molecular turnovers per second. Thus, for a pump site density of 0.125 pmol/cm^2 or 753 sites/μm^2 (Michael et al., 1979; Daut & Rudel, 1981) 1 μA/cm^2 of net pump current corresponds to 82.9 molecular turnovers per second. This means that the constraint on the maximum molecular turnover rate of the enzyme restricts ATPase activity to a maximum equivalent value of 2.01 μA/cm^2.

The set of reactions in Fig. 1 has a total of 12 rate coefficients, of which 11 are independent since the equilibrium constant for the overall reaction is known. It is possible, in principle, to determine values for these rate coefficients by fitting a sufficiently large body of data. In practice and certainly with the limited data available, such a unique set of rate coefficients cannot be determined. Our aim was to find one set of rate coefficients that was consistent with a limited set of experimental data, recognizing that there are other sets that would have also fitted the data. Our findings and conclusions, therefore, must not be considered exhaustive but preliminary. The experimental data were fitted by eye, the choice of rate coefficient(s) to be adjusted to improve the fit being made on the basis of experience.

For voltage-dependent steps, the voltage-dependent rate coefficients were obtained by multiplying the respective rate coefficients by functions of membrane potential, assuming a symmetry factor of 0.5 (*see above*, The Model – Voltage Dependence).

Steady-state solutions for the concentrations of intermediates were obtained by Gaussian elimination and used to solve for the unidirectional rates of each step in the reaction sequence. All equations were solved on a Digital Equipment Corporation VAX 11/780 digital computer with graphical results displayed either on a Tektronix 4006-1 Graphics Display terminal or on a Hewlett-Packard 7221A Graphics Plotter. As a safety check on the computations a 0.01% tolerance was placed on the required agreement between the following pairs of quantities:

1. The sum of the computed enzyme intermediates and the set parameter for total enzyme per unit area of membrane;
2. The overall steady-state rate of reaction defined by Boudart (1976; and *see* footnote 1 on page 148) and the steady-state rate of reaction through step 1;
3. The ratio of the overall unidirectional forward rate of reaction to the overall unidirectional reverse rate of reaction and the ratio predicted thermodynamically from the net free energy dissipation of the overall reaction (Boudart, 1976; Chapman & McKinnon, 1978).

Simulations were performed either vectorially (i.e., true transport across a membrane separating two compartments of different electrochemical composition) or nonvectorially (i.e., isolated enzyme in solution). For the latter case the vectorial computer programs were used with equal concentrations for intracellular and extracellular ionic species and with the membrane potential set equal to zero.

In cases where the effects of varying the ionic concentrations were studied all other electrochemical conditions were held constant unless otherwise stated.

Unidirectional ionic fluxes were calculated by using the method of Boudart (1976) to define unidirectional rates of reaction across steps 1 to 3 of Fig. 1 for Na^+ movements, and across steps 4 to 6 for K^+ movements (*cf.* Chapman, 1982).

Results and Discussion

Nonvectorial ATPase Activity

The behavior of the isolated enzyme in the nonvectorial situation is independent of the choice of voltage-dependent step (*see* The Model – Voltage Dependence) because there is no influence of voltage comparable to the physiological situation in the membrane. There is also no distinction between intracellular and extracellular forms of the ionic species; the two forms of the enzyme capable of reacting with each ionic species are therefore exposed simultaneously to the same bulk concentrations of Na^+ and K^+. Of the available kinetic data we chose to fit those of Skou (1957; 1975) for the activation of the Na^+,K^+-ATPase by Na^+ and K^+ in the presence of saturating levels of ATP. The resulting simulations are shown in Fig. 2*A* (Na^+ activation), 2*B* (K^+ activation), and 2*C* (simultaneous variation of [Na^+] and [K^+]). These Figures should be compared with Figs. 6 and 5 of Skou (1957) and Fig. 1 of Skou (1975), respectively. While certain details of Skou's data cannot be fitted by our scheme (e.g., the Na^+ activation of ATPase in the presence of zero [K^+]), in general the fit is reasonably satisfactory for establishing a working set of rate coefficients.

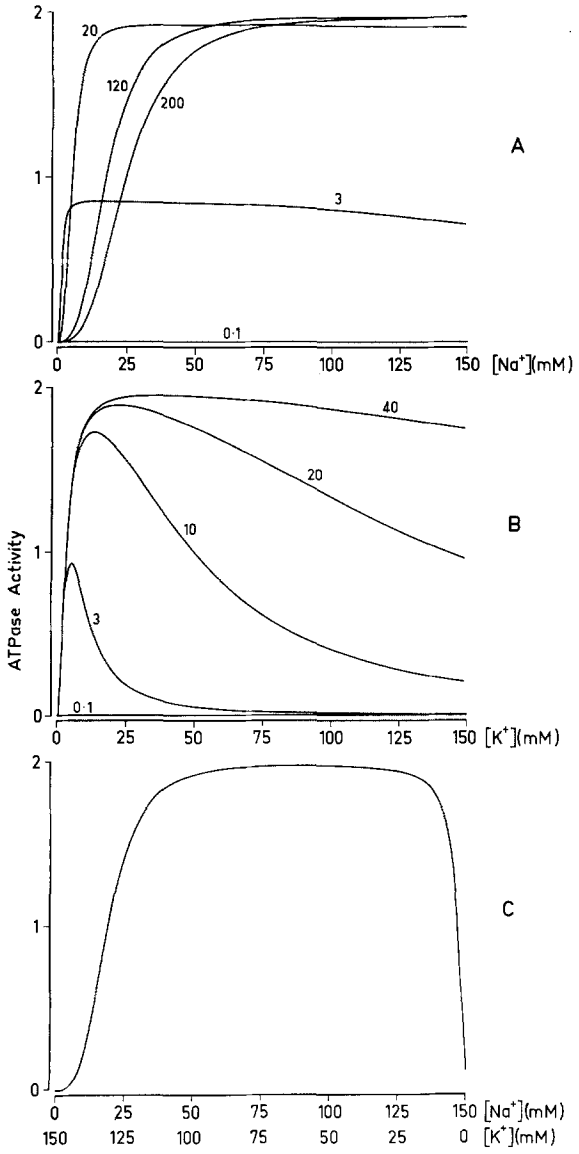

Fig. 2. Activation of nonvectorial ATPase activity by Na^+ and K^+ ions. *A* (upper panel): activation by Na^+ in the presence of different fixed concentrations of K^+ as indicated in mM. *B* (middle panel): activation by K^+ in the presence of different fixed concentrations of Na^+ as indicated in mM. *C* (lower panel): simultaneous activation by Na^+ and K^+ constrained to sum to 150 mM. All rate coefficients and other boundary conditions as in the Table. ATPase activity expressed in μA/cm²; 1 μA/cm² = 82.9 molecular turnovers per second

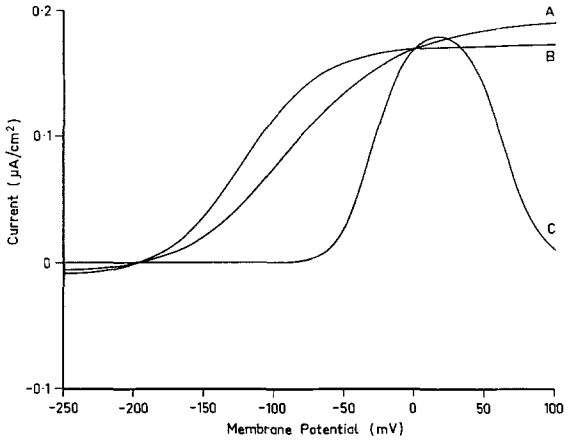

Fig. 3. Pump current-voltage relations for the scheme of Fig. 1 for different locations of the voltage-dependent step(s). *A*: Voltage dependence on step 3; $f_3 = 172\exp(FV/2RT)\text{sec}^{-1}$, $b_3 = 1\cdot72\times10^4\exp(-FV/2RT)$ liter^{3}mol^{-3}sec^{-1}. *B*: Voltage dependence on step 5; $f_5 = 2\times10^6\exp(FV/2RT)$ litermol^{-1}sec^{-1}, $b_5 = 30\exp(-FV/2RT)\text{sec}^{-1}$. *C*: Voltage dependence on steps 3 and 5; $f_3 = 172\exp(3FV/2RT)\text{sec}^{-1}$, $b_3 = 1\cdot72\times10^4\exp(-3FV/2RT)$ liter^{3}mol^{-3}sec^{-1}, $f_5 = 2\times10^6\exp(FV/RT)$ litermol^{-1}sec^{-1}sec^{-1}, $b_5 = 30\exp(-FV/RT)\text{sec}^{-1}$. All other rate coefficients in *A*, *B* and *C* as in the Table

The Pump Current-Voltage Relation

Figure 3 shows the current-voltage (*I–V*) relations obtained when the voltage dependence is assigned to step 3 (*A*), step 5 (*B*), and to both steps 3 and 5 (*C*) as described above (*see* The Model – Voltage Dependence). The same set of rate coefficients (*see* the Table) was used in each case, the values being chosen to yield a satisfactory *I–V* relation for the case of voltage dependence on step 5 while fitting the nonvectorial biochemical data on the isolated enzyme (*see above*). Curves *A* and *B* are quite similar in shape, which suggests that the overall behavior of the model is not critically dependent on which *single* step is chosen to be voltage-dependent. On the other hand, with voltage dependence assigned to both steps, we were unable to find rate coefficients which produced an *I–V* relation like those of curves *A* or *B* of Fig. 3. All *I–V* relations that we could find were of the form shown in curve *C* of Fig. 3, where voltage is a strong inhibitor of transport on either side of a narrow, high conductance region – a relation quite unlike any reported in the physiological literature. Thus, for the remainder of this paper we have assigned the voltage dependence to a single step (5), unless otherwise stated.

It is worth noting that the assignment of the entire voltage dependence to a single reaction step (whichever step is chosen) implies that the entire membrane potential must appear over the reaction distance associated with that step. The choice of 0.5 for the electrical symmetry factor is therefore appropriate (Bockris & Reddy, 1970; Fried, 1973) and does not require justification on the basis of the supposed spatial location of the voltage-dependent step in relation to some supposed continuum distribution of the transmembrane electric field as is sometimes done for carrier-mediated diffusion (Lauger & Stark, 1970; Hall, Mead & Szabo, 1973; Jack, Noble & Tsien, 1975).

It might be suggested that we should have chosen rate coefficients that would give less slope

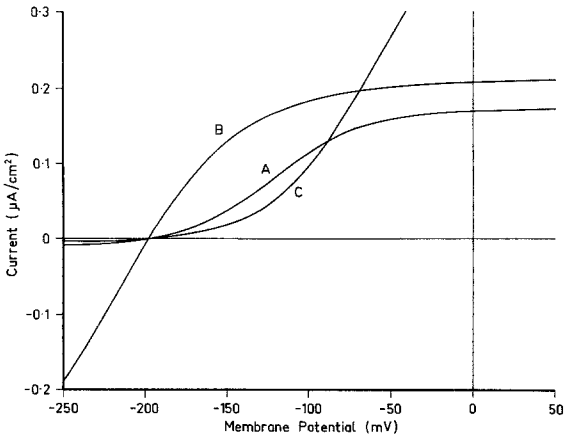

Fig. 4. Pump current-voltage relations with voltage dependence on step 5 of reaction scheme of Fig. 1 as in Fig. 3*B*. *A*: Control. *B*: Rate coefficients adjusted to increase the voltage-dependent reversibility exhibited by curve *A*, $b_2 = 10^7$ liter mol^{-1} sec^{-1}, $f_3 = 1000$ sec^{-1}, $b_3 = 5 \times 10^4$ liter^{3}mol^{-3}sec^{-1}, $f_4 = 10^8$ liter^2 mol^{-2}sec^{-1}, $b_4 = 1 \cdot 33 \times 10^6$ liter mol^{-1}sec^{-1}, $b_5 = \exp(-FV/2RT)$ sec^{-1}, $f_6 = 1 \cdot 91 \times 10^4$ sec^{-1}, all other rate coefficients as in the Table. *C*: Rate coefficients adjusted to reduce the reversibility; $f_5 = 2 \times 10^5 \exp(FV/2RT)$ liter mol^{-1}sec^{-1}, $f_6 = 115$ sec^{-1}, $b_6 = 6 \times 10^5$ liter^{2}mol^{-2}sec^{-1}

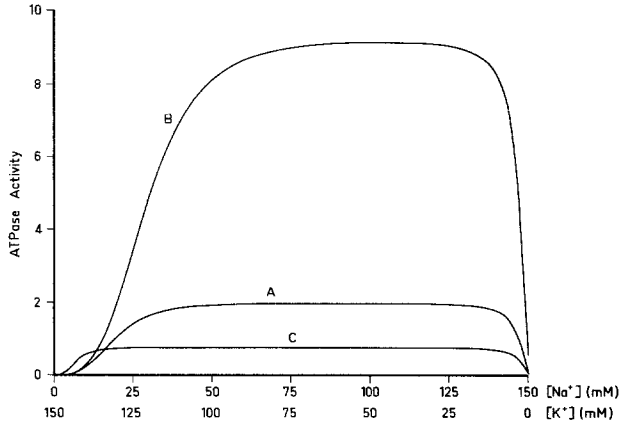

Fig. 5. Simultaneous activation of nonvectorial ATPase activity by Na^+ and K^+ ions constrained to sum to 150 mM, using the rate coefficients yielding the current-voltage relations of Figs. 4*A*, *B* and *C*, respectively. ATPase activity expressed in μA/cm^2; 1 μA/cm^2 = 82.9 molecular turnovers per second

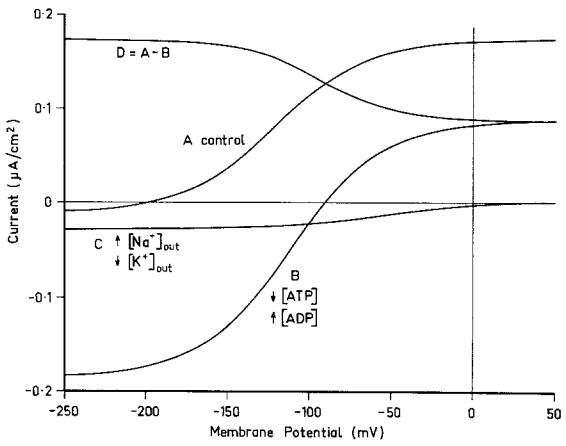

Fig. 6. Effect of altered chemical conditions on the pump current-voltage relation. *A*: Control; rate coefficients and parameters as in the Table. *B*: Effect of reducing [ATP] from 4.99 mM (control) to 3.0 mM with corresponding increase in [ADP]; other rate coefficients and parameters as in the Table. *C*: Effect of increased ionic concentration gradients; extracellular [Na^+] increased to 200 mM and extracellular [K^+] lowered to 0.1 mM; all other rate coefficients and parameters as in the Table. *D*: The difference between curve *A* (control) and curve *B* (reduced free energy available from ATP splitting)

conductance in the physiological range than evident in Fig. 3*B*. However, there are two interacting properties to be weighed against each other: the relative slope conductance in the physiological range versus the relative reversibility of the pump beyond the reversal potential. By the latter we mean the relative magnitude of the pump current at potentials beyond (more negative than) the reversal potential compared to that at potentials positive to the reversal potential. As is illustrated in Fig. 4, we found that the condition of less physiological slope conductance (curve *B*) is associated with a relatively high degree of voltage-dependent reversal; conversely, a larger physiological slope conductance (curve *C*) is associated with relatively little voltage-dependent reversal. Although we have pointed out before that a pump reversal potential must exist on thermodynamic grounds (Chapman & Johnson, 1978), no significant reversal of electrogenic transport currents has been reported. For this reason we have chosen the compromise relation (Fig. 4*A* or 3*B*) as our control in subsequent simulations.

Moreover, the choices of rate coefficients yielding the *I–V* curves of Fig. 4*B* and *C* result in significant alterations to the nonvectorial activation behavior of the isolated ATPase as shown in Fig. 5*B* and *C*, respectively. Although the rate coefficients for Fig. 4*B* fall within the constraints listed earlier (*see* Materials and Methods) the maximum turnover number of the isolated enzyme has become unacceptably large in Fig. 5*B*. On the other hand, the rate coefficients for Fig. 4*C* produce an unacceptable diminution and change in shape of the enzymatic activation curve in Fig. 5*C*. This suggests that the seemingly unlimited freedom in choosing appropriate rate coefficients for the six steps of Fig. 1 might become quite restricted when all known physiological and biochemical requirements are taken into account.

Gradman et al. (1981) have suggested that an *I–V* curve which exhibits little voltage-dependent reversal, such as that of Fig. 4*A*, reflects the possibility that voltage may be kinetically incompetent to synthesize ATP. This is not necessarily true:

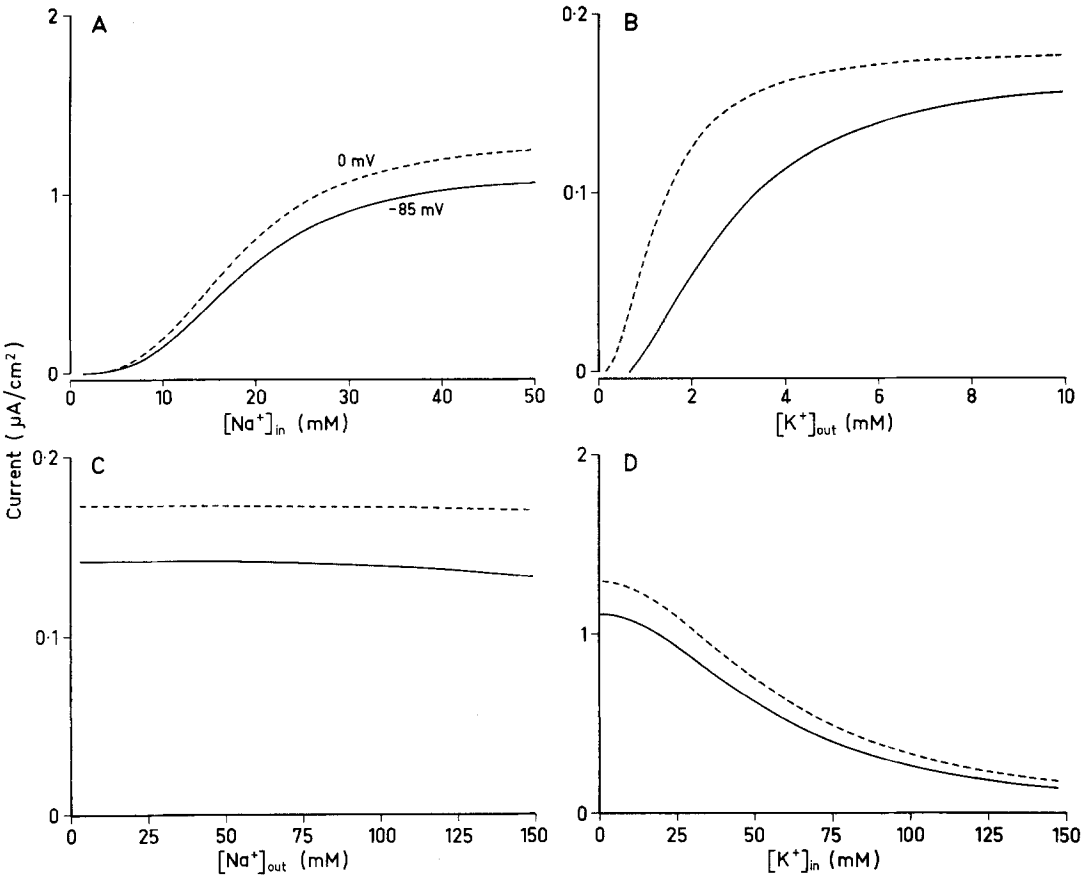

Fig. 7. Activation of vectorial ATPase activity (electrogenic pump current) by intracellular and extracellular Na^+ and K^+ at membrane potentials of zero (broken lines) and −85 mV (solid lines). *A*: Activation by Na^+_{in}. *B*: Activation by K^+_{out}. *C*: Inhibition by Na^+_{out}. *D*: Inhibition by K^+_{in}. All other rate coefficients and parameters as in the Table

Figure 6 illustrates that such relative irreversibility totally disappears when the ATP concentration is reduced (with a corresponding increase in ADP concentration) from 4.99 (*A*) to 3.0 mM (*B*), a condition similar to that in which pump reversal was first demonstrated in red cells by Garrahan and Glynn (1967*b*). As Fig. 6*B* shows, under these conditions voltage may become a powerful force resulting in synthesis of ATP. Gradmann et al. (1981) also suggested that an increased ion concentration gradient might produce more significant pump reversal than imposition of a voltage gradient. However, this prediction is not borne out by the behavior of the present model, where simultaneous raising of Na^+_{out} to 200 mM and lowering of K^+_{out} to 0.1 mM at normal ATP levels simply reduces the forward rate of reaction without significantly enhancing the reverse rate despite a huge shift in the reversal potential (*see* Fig. 6*C*).

The Ionic Dependences of the Transport Rates

Most of the dependences of the transport rate on chemical composition have been determined under conditions where the membrane potential was not controlled. Consequently, the published data are necessarily confounded by the possible effects of voltage as well as ionic concentration on the transport rates. Figures 7*A* and *B* show the activation by intracellular Na^+ and extracellular K^+, respectively, at −85 and 0 mV. Similarly, Figs. 7*C* and *D* show inhibition by extracellular Na^+ and intracellular K^+, respectively, at −85 and 0 mV. The effect of voltage can be seen for all four ionic dependences, altering the K_m's for activation by intracellular Na^+ or extracellular K^+, and that for inhibition by intracellular K^+. It is interesting to note that, with regard to activation by extracellular K^+, voltage here produces the largest shift of the K_m but only a moderate change in maximal rate. Since, in the absence of voltage control, an increase in extracellular $[K^+]$ produces depolarization, one might expect the experimental activation curve to shift from the solid line (−85 mV) to the broken line (0 mV) as the extracellular $[K^+]$ is raised.

The sigmoidal relation for activation by intracellular Na^+ (Fig. 7*A*) is consistent with the experimental finding of an approximately first-order ac-

tivation of electrogenic pump current over the physiological range of intracellular [Na^+] (approximately 10 to 20 mM) in dog Purkinje fibers (Gadsby & Cranefield, 1979*a*). Keynes and Swan (1959) and Mullins and Frumento (1963) reported a saturating cubic activation by intracellular Na^+ in frog muscle, corresponding to the wider range of intracellular [Na^+] shown in the curves of Fig. 7*A*. Similar activation by $[Na^+]_{in}$ was found in red cells by Garay and Garrahan (1973). Brinley and Mullins (1968) found a linear activation of unidirectional transport-mediated Na^+ efflux in squid axon over a wide range of intracellular [Na^+], a finding not in accord with Fig. 7*A*. However, measurement of unidirectional fluxes can be an unreliable measure of net transport (Chapman, 1982) as discussed below.

A K_m of about 1 mM for activation of electrogenic pump current by extracellular K^+ has been reported by Gadsby and Cranefield (1979*b*) for dog Purkinje fibers with the membrane potential held at around −30 mV. Garrahan and Glynn (1967*a*) found a K_m for the extracellular K^+-activated Na^+/K^+ exchange in red cells of just over 1 mM [K^+]. These findings accord with the behavior of our model with little or no membrane potential but not with a membrane potential of the order of −85 mV (*see* Fig. 7*B*).

The relative insensitivity of net Na^+/K^+ transport to extracellular Na^+ is consistent with a wide range of physiological observations. Lowering external [Na^+] has little effect on Na^+ efflux from red cells into normal K^+-containing medium (Garrahan & Glynn, 1967*a*). The absence of marked hyperpolarization in excitable cells in low [Na^+] media is also in keeping with the relatively weak influence of extracellular Na^+ on Na^+/K^+ pump current. Such insensitivity is one of the more important differences between the present model and the one used previously (Chapman et al., 1979). In that model, transport was treated as an 'elementary-complex' reaction, where an assumed saturation of the reverse rate of reaction by external Na^+ forced an inverse third-order dependence of the forward rate. As a consequence, relatively mild reductions of external [Na^+] produced enormous increases in pump current with unrealistic hyperpolarizations of the membrane potential.

The strong inhibitory effect of intracellular K^+ on net transport (Fig. 7*D*) is a direct consequence of fitting the nonvectorial K^+ activation behavior to that described by Skou (1957). In the present model the inhibition by intracellular K^+ is due to competition with intracellular Na^+ for combination with the E·ATP form of the enzyme. The reason that extracellular Na^+ does not show an

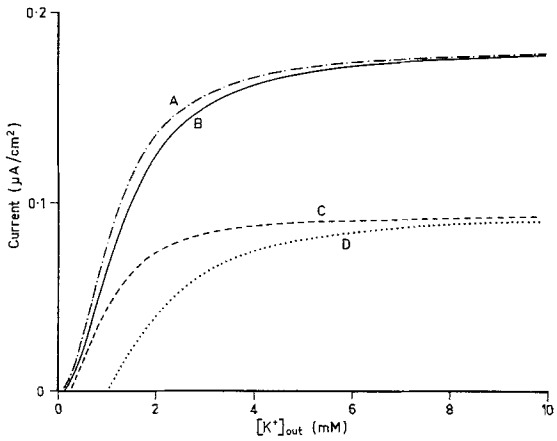

Fig. 8. Activation of Na^+/K^+ transport by K^+_{out} with [ATP] set at 4.99 mM (*A* and *B*) or 3.0 mM (*C* and *D*) and $[Na^+]_{out}$ set at 140 mM (*B* and *D*) or 50 mM (*A* and *C*). All other rate coefficients and parameters as in the Table with [ATP]+[ADP] constrained to sum to 5.05 mM

equal inhibitory effect by competing with extracellular K^+ for combination with the E′−P form of the enzyme is a consequence of our choices of rate coefficients for the first three steps which cause the the model to exhibit little Na^+/Na^+ exchange at normal ATP levels. Consequently, the behavior of the present model is unlike that of the sodium pump of red cells but more like that of squid axon, where Na^+/Na^+ exchange appears only when the energy available from ATP is reduced (Caldwell, Hodgkin, Keynes & Shaw, 1960; *see also* Fig. 9). In that case the steps involving Na^+ extrusion become more reversible and the model now exhibits competition between extracellular Na^+ and K^+ for combination with the E′−P form of the enzyme. Figure 8 shows activation of Na^+/K^+ transport by extracellular K^+ at normal (*B* and *D*) and reduced (*A* and *C*) extracellular [Na^+], for normal (*A* and *B*) and reduced (*C* and *D*) energy available from ATP. Reduction of [ATP] by 40% reduces the maximum rate of transport but also has a striking effect on the kinetics of activation by K^+_{out}, greatly increasing the 'inhibition' by Na^+_{out} at low [ATP].

Unidirectional Fluxes

It has been shown previously that unidirectional fluxes, such as can be measured isotopically in rapid dialysis experiments, are generally useless for establishing the stoichiometry of a transport reaction involving a sequence of elementary steps (Chapman, 1982). Furthermore, the unidirectional flux of isotope through such a sequence of steps is not a measure of the steady-state overall unidirectional rate of reaction as defined by Boudart

(1976)[1]. This is because the steady-state overall rate of reaction can only be measured by labeling a molecule or ion that enters exclusively at the first elementary step in the sequence and emerges equally exclusively at the last elementary step in the sequence. In the scheme of Fig. 1 no such labeling is possible for any of the reactants; nor is it possible to conceive of labeling one form of the enzyme, since any form of the enzyme can be consumed and generated by both forward and backward progress through the six steps.

Because of these considerations it is to be expected that unidirectional fluxes of isotope will be generally uninterpretable without prior knowledge of the number and stoichiometry of the intermediate steps in the overall reaction. This is strikingly illustrated by plots of unidirectional fluxes versus voltage such as those shown in Fig. 9. Results at potentials extending beyond the normal physiological range are shown in order to illustrate that the voltage dependence of a unidirectional flux (in this case K^+ influx) can bear no obvious relation to voltage-dependent ATPase activity or to net Na^+/K^+ transport. In this particular example there is a good correlation between unidirectional Na^+ efflux and net transport because of the relative irreversibility of the first three steps and the absence thereby of Na^+/Na^+ exchange (Fig. 9*A*). On the other hand, when chemical conditions are altered (e.g., 40% reduction of [ATP]), marked Na^+/Na^+ exchange appears as shown in Fig. 9*B*.

Note that the control peak value of Na^+ extrusion in Fig. 9 is three times the value of the peak control current in Fig. 3*B* owing to the pump stoichiometry of 3 Na^+ extruded per unit charge transferred.

It is a corollary of the results of Fig. 9 that unidirectional flux measurements cannot be used, via the thermodynamic rate-ratio equation, to estimate thermodynamic quantities such as the free energy of ATP splitting as had been suggested earlier (Chapman, 1973). The failure of the rate-ratio equation to be useful in this context is not due to a breakdown in the theoretical relation between kinetic and thermodynamic data (Boudart, 1976), but to a failure of experimental methods to provide a true measure of the unidirectional rates of active transport.

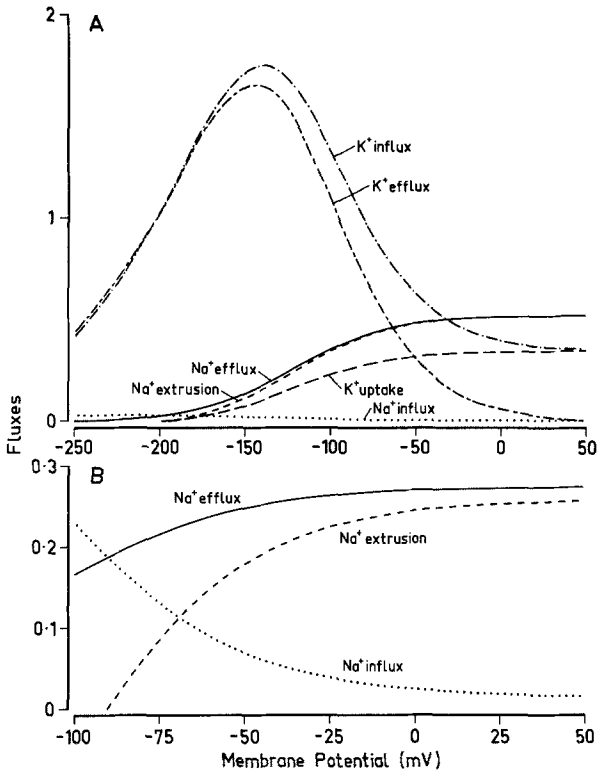

Fig. 9. Unidirectional (isotopic) and net fluxes of Na^+ and K^+ as a function of membrane potential. *A*: Control; rate coefficients and parameters as in the Table; note absence of significant Na^+/Na^+ exchange over most of the range. *B*: Unidirectional and net fluxes of Na^+ with [ATP] reduced from 4.99 mM (control) to 3.0 mM to increase the reversibility of step 2 of Fig. 1; note presence of large amounts of Na^+/Na^+ exchange. [ATP]+[ADP] constrained to sum to 5.05 mM; all other rate coefficients and parameters as in the Table. Fluxes expressed in electrical units of $\mu A/cm^2$

While not providing a measure of overall reaction rate, unidirectional ion flux measurements do provide information about the exchange of transported species through various intermediate steps of the reaction mechanism. However, the exchange occurs because of the microscopic reversibility of each elementary step; it does not represent alternative modes of enzyme action for the transport ATPase. Recognizing the essential identity between vectorial and nonvectorial chemical reactions at the molecular level (Mitchell, 1977), it is clear that any quantitative discrepancy between the unidirectional rate and the net rate through a series of elementary steps under different conditions is simply a measure of the degree of reversibility of those steps, not of the number of possible chemical reactions that the system might catalyze under different conditions. Therefore, it is absolutely neces-

[1] The overall steady-state unidirectional rates of forward and reverse reaction for the scheme of Fig. 1 are, following Boudart (1976):

$$r_f = rf_1 \cdot rf_2 \cdot rf_3 \cdot rf_4 \cdot rf_5 \cdot rf_6/d$$

$$r_b = rb_1 \cdot rb_2 \cdot rb_3 \cdot rb_4 \cdot rb_5 \cdot rb_6/d$$

where

$$d = rf_2 \cdot rf_3 \cdot rf_4 \cdot rf_5 \cdot rf_6 + rb_1 \cdot rf_3 \cdot rf_4 \cdot rf_5 \cdot rf_6 + rb_1 \cdot rb_2 \cdot rf_4 \cdot rf_5 \cdot rf_6 + rb_1 \cdot rb_2 \cdot rb_3 \cdot rf_5 \cdot rf_6 + rb_1 \cdot rb_2 \cdot rb_3 \cdot rb_4 \cdot rf_6 + rb_1 \cdot rb_2 \cdot rb_3 \cdot rb_4 \cdot rb_5$$

and the rf_i, rb_i are the forward and reverse mass action rates of the i^{th} elementary step of Fig. 1.

sary to determine and subtract the pump 'exchange' fluxes before using unidirectional pump flux data to estimate overall reaction velocities.

Saturation of Enzyme and Reaction Rates

Since we have assumed, to begin with, that all of the enzyme is complexed with one or more of the reactants and products, the nearest analogy to 'free' enzyme would be the complex we have designated 'E·ATP'. Thus, the fraction of total enzyme not in the form of E·ATP might be taken to represent the degree of 'saturation' of the total amount of enzyme available. Figures 10*A*, *B* and *C* are plots of intermediate composition corresponding to the voltage and chemical dependences illustrated in Figs. 3*B*, 7*A* and 7*B*, respectively. The dependences of net transport on voltage and chemical composition are certainly not the result of changes in the amount of E·ATP available which, for the parameters yielding these Figures, is negligible at all voltages and ionic concentrations.

The only other form of the enzyme not complexed with Na^+ or K^+, i.e., E′—P, shows a decline in concentration as the transport rate is activated by voltage (Fig. 10*A*) or K^+_{out} (Fig. 10*C*), but shows an increase in concentration for activation by Na^+_{in} (Fig. 10*B*).

In the classic treatment of an enzyme reaction as a single reversible elementary step to form an enzyme-substrate complex, followed by an irreversible formation of products, saturation of the forward rate of reaction is identical with, and due to, saturation of the enzyme. No such simple relation obtains, however, for a sequence of reversible elementary steps, such as those of Fig. 1. As the results of Fig. 10 clearly show, the voltage and chemical dependences of the reaction rates that are illustrated in Figs. 2 through 9 arise, not from a changing degree of saturation of the total amount of enzyme, but from a shifting balance between the various enzyme forms represented by the six intermediates.

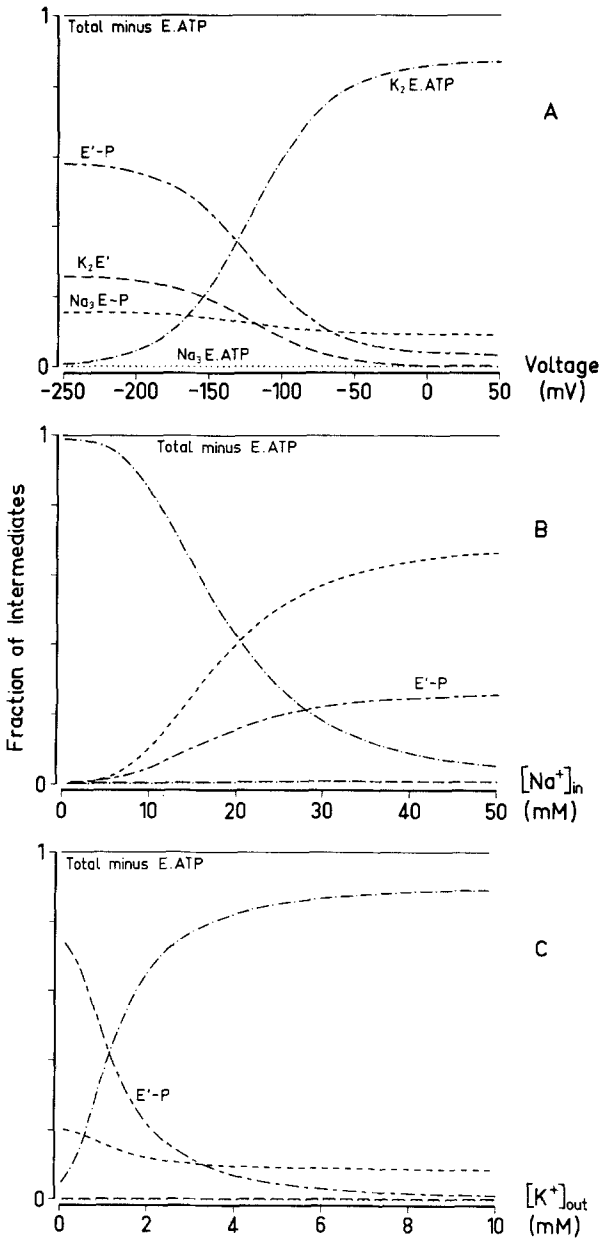

Fig. 10. Distribution of concentrations of enzyme intermediates as fractions of total enzyme versus membrane potential (*A*), intracellular $[Na^+]$ (*B*) and extracellular $[K^+]$ (*C*). All rate coefficients and parameters as in the Table

Voltage-Dependent Binding of Na^+ and K^+

The distributions of intermediates shown in Fig. 10 contain information about the proportions of enzyme binding Na^+ and K^+ ions. With all of the voltage dependence assigned to step 5 of the scheme of Fig. 1 it follows that no step involving binding or dissociation between Na^+ or K^+ and the enzyme is directly influenced by voltage. However, there is a considerable indirect effect of voltage on the binding of Na^+ or K^+ to the enzyme, owing to the voltage-dependent distribution of intermediates. Figure 11 illustrates how the respective proportions of enzyme to which Na^+ and K^+ are bound change as the membrane potential is varied.

Free Energy Dissipation and Conservation

The free energy available from the splitting of ATP is the potential energy difference that drives net transport of Na^+ and K^+ ions. Some of this energy is conserved in the electrochemical work of ion translocation; the remainder is dissipated in producing net reaction at *each* of the six reaction steps. For example, Fig. 12*A* shows how this dissipation

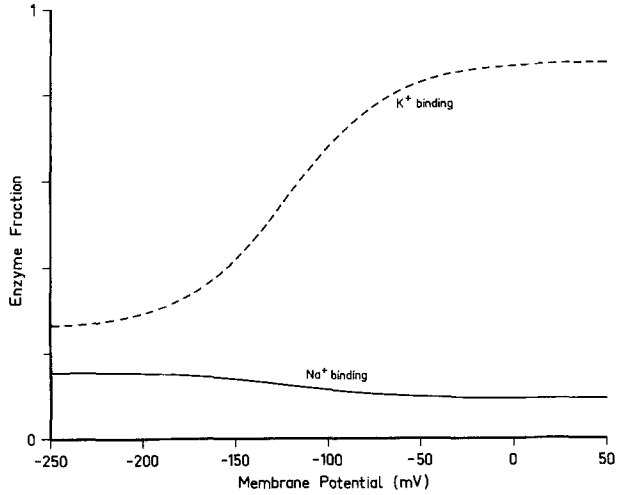

Fig. 11. Summed distribution of enzyme intermediate forms binding Na^+ and K^+ versus membrane potential. All rate coefficients and parameters as in the Table

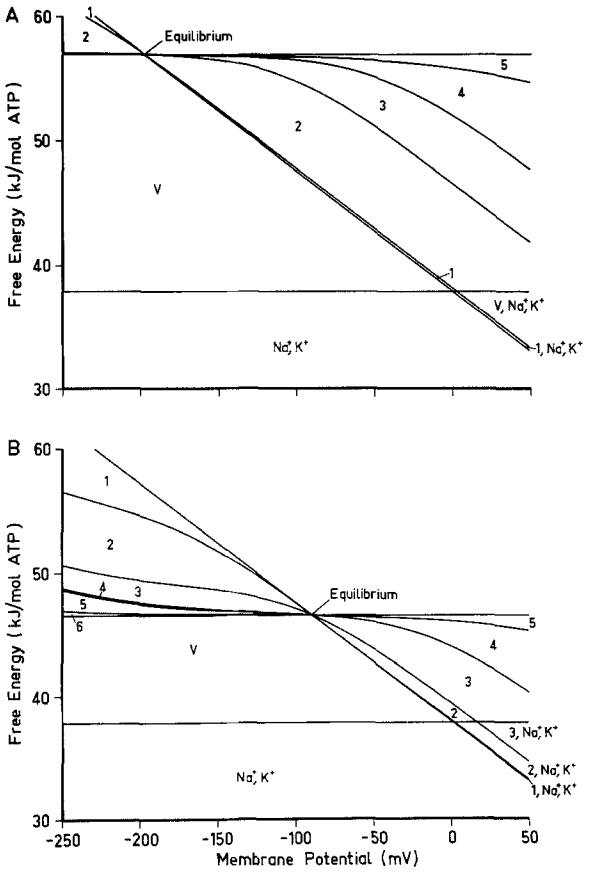

Fig. 12. Conservation and dissipation of the free energy available from ATP splitting as a function of membrane potential. Curves plotted sequentially as the cumulative sum of the following: $3RT\ln([Na^+]_{out}/[Na^+]_{in})+2RT\ln([K^+]_{in}/[K^+]_{out})$; $-FV$; $RT\ln(rf_i/rb_i)$ for $i=1$ through 6 for each of the elementary steps of the scheme of Fig. 1. *A*: Control. *B*: [ATP] reduced to 3 mM with corresponding increase in [ADP]. All other parameters and rate coefficients as in the Table. Note the truncated ordinates and that all free-energy dissipation and conservation terms sum to the corresponding free energy of ATP splitting. Also, the voltage term becomes dissipative for membrane potentials greater than zero (inside positive) while all the rate-dependent dissipation terms converge to zero and intersect at the pump reversal potential

is distributed over these steps as a function of membrane potential. Most of the energy dissipation is across steps 2 and 3 at normal physiological potentials, with significant dissipation occurring at steps 4 and 5 only at extreme depolarizations. That is to say, steps 2 and 3 are normally the reactions most far removed from thermodynamic equilibrium. Steps 1 and 6 are very close to thermodynamic equilibrium at all potentials. The fact that step 2, one of the essential steps in any possible Na^+/Na^+ exchange, is so irreversible (i.e., highly dissipative) explains why the model with the given rate coefficients and boundary conditions displays no significant Na^+/Na^+ exchange.

Leaving the rate coefficients unchanged, this distribution is greatly altered when the level of ATP is reduced. The resultant increase in the level of ADP produces backward pressure on step 2, increasing its reversibility as reflected in the energy curves shown in Fig. 12*B* for a 40% reduction of [ATP].

Note in both graphs of Fig. 12 that the horizontal line representing the summated conserved and dissipated free energies corresponds to the respective free energy available from ATP splitting.

These curves thus illustrate how the free energy available from ATP splitting might be partitioned between conservation in the electrochemical work of ion translocation and dissipation at the various elementary steps along the reaction sequence. For the particular rate coefficients we have chosen, some of these steps are always close to thermodynamic equilibrium (e.g., steps 1 and 6) while others are far removed from equilibrium (e.g., steps 2 and 3) and thereby account for much of the free-energy dissipation.

Electrophysiological Implications

The Steady State. It is clear from the curves of Fig. 4 that, regardless of the choice of rate coefficients or relative reversibility of the pump under physiological concentrations of ATP

and ionic species, there must be a range of membrane potentials over which the pump mechanism displays considerable slope conductance. The fact that no reports of such a contribution by the pump to the total membrane slope conductance exist in the literature indicates that this range of membrane potentials lies normally beyond the limits of hyperpolarization in electrophysiological experiments. On the other hand, as we have suggested previously (Chapman & Johnson, 1978), this behavior might well be brought into the experimental range of membrane potentials by reducing the free energy available from ATP splitting (*see* Fig. 6).

In our previous model (Chapman et al., 1979) the high degree of pump reversibility immediately beyond the resting potential (hyperpolarizing) led to a high pump contribution to the membrane slope conductance. This was due to two factors: (a) our use of older values from the literature for the free energy available from ATP splitting (magnitude less than -50 kJ/mol ATP) and (b) our forcing all of the voltage dependence on to the reverse rate of a single 'elementary-complex' reaction (*see above,* The Model – Voltage Dependence). Using more modern estimates of the free energy of ATP splitting (Hassinen & Hiltunen, 1975; Veech et al., 1979) places the pump reversal potential around 100 mV more negative than the resting potential. With our earlier treatment of the pump as a single 'elementary-complex' reaction this would have removed any possibility of the pump contributing to the membrane slope conductance in the physiological range. However, the effects of redistribution of intermediates in the present multi-step enzymatic model with changes in membrane potential (Fig. 11) cause the voltage dependence of net transport to be spread to potentials far distant from the reversal potential.

Indeed, the inclusion of several intermediate steps in the pump mechanism allows a single voltage-dependent step to result in a wide range of possible *I–V* curves of potentially complex shape, some of which have been explored by Gradmann et al. (1981) and Hansen et al. (1981). Therefore, it would seem of paramount importance to our understanding of the contribution of electrogenic transport to electrophysiology that the pump *I–V* relation should be determined accurately. Unfortunately, the geometry and morphology of most cellular preparations make it impossible to control adequately the chemical composition of intracellular and extracellular space before and after the pharmacological or metabolic blockades usually employed to separate active Na^+/K^+ transport current from passive and other transport/exchange currents.

Moreover, the experimental technique of poisoning the ATP supply system is wholly inadequate as a means of eradicating the contribution of active electrogenic transport to the membrane *I–V* relationship. This is because the pump is likely to become highly reversible when ATP is depleted and ADP accumulates, resulting in 'difference' *I–V* curves (i.e., before and after metabolic blockade) that have no reversal potential (*see* curve *D* of Fig. 6). While it must be admitted that the adenylate kinase system, together with deamination of adenosine monophosphate, would tend to buffer the accumulation of ADP in poisoned cells (Atkinson, 1977), the fact remains that any increase at all in ADP concentration would enhance the reverse rate of electrogenic transport beyond the reversal potential and thereby render invalid the subtraction of membrane I–V curves before and after poisoning.

Transient Responses. All of the simulations presented here have been steady-state solutions of the differential equations describing rates of changes of enzyme intermediates. Clearly, the response to a step change in transmembrane potential will not be instantaneous. Time will be required for the intermediates to change from one steady-state distribution to another (e.g., *see* voltage-dependent distribution of intermediates shown in Fig. 10 *A*). If more than one rate-limiting step exists in the overall sequence, then the time constants of those reactions will determine the time-dependence of the pump current in response to a change in membrane potential. For the normal physiological values in the present scheme at a resting potential of -85 mV the pseudo first-order time constants of the slowest steps are 4.6, 0.7 and 0.5 msec for steps 3, 4 and 5, respectively. For the assumed pump site density of 0.125 pmol/cm^2 the total charge transferred per unit of membrane capacitance (1 μF/cm^2) amounts to 12 mV per cycle of overall reaction. Consequently, one might expect the charged forms of the Na^+,K^+-ATPase to contribute significantly to experimentally observable charge displacement or pseudo 'gating' currents on a time scale similar to those that might be observed in connection with the fast Na^+ conductance responsible for the upstroke of the cardiac action potential following steps in membrane voltage.

The Molecular Reaction Mechanism

It has not been the purpose of the present paper to vindicate or support any particular reaction scheme for the Na^+,K^+-ATPase. Our choice of the scheme of Fig. 1 derives from its unequivocal stoichiometric formulation which allows detailed computer simulation of its possible biochemical and physiological behavior. The scheme is clearly an oversimplification for we have assumed that the three Na^+ ions, or the two K^+ ions, react with the enzyme simultaneously. In our view the literature presenting proposed mechanisms for the Na^+,K^+-ATPase is alarmingly bereft of stoichiometric coefficients for Na^+ and K^+ at the various points of entry and exit in the reaction sequence. The scheme summarized by Guidotti (1979) which we have adopted with slight modification (Fig. 1) is explicit in its stoichiometric formulation.

The set of rate coefficients listed in the Table is certainly only one of many possible sets that would enable the scheme of Fig. 1 to generate data similar to those presented here. However, it is clear from the present work that the constraints listed earlier do limit the range of permissible values for the rate coefficients, and there are significant consequences for the biochemical behavior of the model if the rate coefficients are altered to change the electrophysiological behavior, and vice versa.

As it stands, the scheme of Fig. 1 falls into the 'ping-pong' class of molecular mechanism and so its behavior conflicts with the kinetic studies of Hoffman and Tosteson (1971), Garay and Garrahan (1973), Chipperfield and Whittham (1974) and Sachs (1977). The question as to whether the true ATPase mechanism actually occurs according to this type of 'ping-pong' mechanism as distinct from an overlapping of binding of Na^+ and K^+ to the enzyme (whether sequential or simultaneous) is one that can be addressed by the methods used in this paper.

The speed and availability of digital computers now permit almost unrestricted quantitative testing of kinetic schemes and interpretative ideas concerning biological transport processes. Differential equations expressing the laws governing the behavior of known or postulated components of a given system can be written and solved without necessary recourse to tractable analytic expressions evolved out of necessity in the absence of fast computers. To this extent there is no longer any need to persist with simplifying mathematical devices (e.g., idealized Michaelis-Menten schemes, linear nonequilibrium thermodynamics, 'elementary-complex' reactions) to analyze complex biological transport systems.

We are greateful to Drs. Jacqueline Reynolds and Charles Tanford for valuable discussion and critical comment. This work was supported by a Grant-in-Aid from the National Heart Foundation of Australia (G1490).

References

Atkinson, D.E. 1977. Cellular Energy Metabolism and its Regulation. Academic Press, New York

Attwell, D., Cohen, I., Eisner, D.A. 1979. Membrane potential stability conditions for a cell with a restricted extra-cellular space. *Proc. R. Soc. London B* **206**:145–161

Bockris, J.O'M., Reddy, A.K.N. 1970. Modern electrochemistry: An Introduction to an Interdisciplinary Area. Plenum Press, New York

Boudart, M. 1976. Consistency between kinetics and thermodynamics. *J. Phys. Chem.* **80**:2869–2870

Brinley, F.J., Mullins, L.J. 1968. Sodium fluxes in internally dialyzed squid axons. *J. Gen. Physiol.* **52**:181–211

Brown, H., Di Francesco, D., Noble, D., Noble, S. 1980. The contribution of potassium accumulation to outward currents in frog atrium. *J. Physiol. (London)* **306**:127–149

Caldwell, P.C., Hodgkin, A.L., Keynes, R.D., Shaw, T.I. 1960. Partial inhibition of the active transport of cations in the giant axons of *Loligo*. *J. Physiol. (London)* **152**:591–600

Chapman, J.B. 1973. On the reversibility of the sodium pump in dialyzed squid axons. A method for determining the free energy of ATP breakdown? *J. Gen. Physiol.* **62**:643–646

Chapman, J.B. 1982. A kinetic interpretation of "variable" stoichiometry for an electrogenic sodium pump obeying chemiosmotic principles. *J. Theor. Biol.* **95**:665–678

Chapman, J.B. 1983. Thermodynamics and kinetics of electrogenic pumps. *In:* Electrogenic Transport. Fundamental Principles and Physiological Implications. M.P. Blaustein and M. Lieberman, editors. Raven Press, New York (*in press*)

Chapman, J.B., Johnson, E.A. 1978. The reversal potential for an electrogenic sodium pump: A method for determining the free energy of ATP breakdown? *J. Gen. Physiol.* **72**:403–408

Chapman, J.B., Kootsey, J.M., Johnson, E.A. 1979. A kinetic model for determining the consequences of electrogenic active transport in cardiac muscle. *J. Theor. Biol.* **80**:405–424

Chapman, J.B., McKinnon, I.R. 1978. Consistency between thermodynamics and kinetic models of ion transport processes. *Proc. Aust. Soc. Biophys.* **2**:3–7

Chapman, K.M. 1980. The sodium pump as a current source: Linear thermodynamic equations for the transmembrane potential and its transient responses to changes in transport rate. *Physiologist* **76**:18a

Chipperfield, A.R., Whittham, R. 1974. Evidence that ATP is hydrolysed in a one step reaction of the sodium pump. *Proc. R. Soc. London B* **187**:269–280

Daut, J., Rudel, R. 1981. Cardiac glycoside binding to the Na/K-ATPase in the intact myocardial cell: Electrophysiological measurement of chemical kinetics. *J. Mol. Cell. Cardiol.* **13**:777–782

Fried, I. 1973. The chemistry of electrode processes. Academic Press, London

Gadsby, D.C., Cranefield, P.F. 1979*a*. Direct measurement of changes in sodium pump current in canine cardiac Purkinje fibers. *Proc. Natl. Acad. Sci. USA* **76**:1783–1787

Gadsby, D.C., Cranefield, P.F. 1979*b*. Electrogenic sodium extrusion in cardiac Purkinje fibers. *J. Gen. Physiol.* **73**:819–837

Garay, R.P., Garrahan, P.J. 1973. The interactions of sodium and potassium with the sodium pump in red cells. *J. Physiol. (London)* **231**:297–325

Garrahan, P.J., Glynn, I.M. 1967*a*. Factors affecting the relative magnitudes of the sodium:potassium and sodium:sodium exchanges catalysed by the sodium pump. *J. Physiol. (London)* **192**:189–216

Garrahan, P.J., Glynn, I.M. 1967*b*. The incorporation of inorganic phosphate into adenosine triphosphate by reversal of the sodium pump. *J. Physiol. (London)* **192**:237–256

Gradmann, D., Hansen, U.-P., Slayman, C.L. 1981. Reaction kinetic analysis of current-voltage relationships for electrogenic pumps in *Neurospora* and *Acetabularia*. *Curr. Top. Membr. Transp.* **16**:257–276

Guidotti, G. 1979. Coupling of ion transport to enzyme activity. *In:* The Neurosciences, Fourth Study Program. I.O. Schmitt and F.G. Worden, editors. pp. 831–840. MIT Press, Boston, Mass.

Hall, J.E., Mead, C.A. Szabo, G. 1973. A barrier model for current flow in lipid bilayer membranes. *J. Membrane Biol.* **11**:75–97

Hammes, G.G., Schimmel, P.R. 1970. Rapid reactions and transient states. *In:* The Enzymes, 3rd ed. P.D. Boyer, editor. Vol. II, Ch. 2. Academic Press, New York

Hansen, U.-P., Gradmann, D., Slayman, C.L. 1981. Interpretation of current-voltage relationships for "active" ion transport systems: I. Steady-state reaction-kinetic analysis of class-I mechanisms. *J. Membrane Biol.* **63**:165–190

Hassinen, I.E., Hiltunen, K. 1975. Respiratory control in isolated perfused rat heart. Role of the equilibrium relations between the mitochondrial electron carriers and the adenylate system. *Biochim. Biophys. Acta* **408**:319–330

Hoffman, P.G., Tosteson, D.C. 1971. Active sodium and potassium transport in high potassium and low potassium sheep red cells. *J. Gen. Physiol.* **58**:438–466

Jack, J.J.B., Noble, D., Tsien, R.W. 1975. Electric current flow in excitable cells. Oxford University Press, Oxford

Jakobsson, E. 1980. Interactions of cell volume, membrane potential, and membrane transport parameters. *Am. J. Physiol.* **238**:C196–C206

Johnson, E.A., Chapman, J.B., Kootsey, J.M. 1980. Some electrophysiological consequences of electrogenic sodium and potassium transport in cardiac muscle: A theoretical study. *J. Theor. Biol.* **87**:737–756

Jorgensen, P.L. 1980. Sodium and potassium ion pump in kidney tubules. *Physiol. Rev.* **60**:864–917

Keizer, J. 1975. Thermodynamic coupling in chemical reactions. *J. Theor. Biol.* **49**:323–335

Keynes, R.D., Swan, R.C. 1959. The effect of external sodium concentration on the sodium fluxes in frog skeletal muscle. *J. Physiol. (London)* **147**:591–625

Kootsey, J.M., Johnson, E.A., Chapman, J.B. 1981. Electrochemical inhomogeneity in ungulate Purkinje fibers: Model of electrogenic transport and electrodiffusion in clefts. *Adv. Physiol. Sci.* **8**:83–92

Lauger, P., Stark, G. 1970. Kinetics of carrier-mediated ion transport across lipid bilayer membranes. *Biochim. Biophys. Acta* **211**:458–466

Lieberman, M., Sawanobori, T., Kootsey, J.M., Johnson, E.A. 1975. A synthetic strand of cardiac muscle. Its passive properties. *J. Gen. Physiol.* **65**:527–550

Michael, L.H., Schwartz, A., Wallick, E.T. 1979. Nature of the transport adenosine triphosphatase-digitalis complex: XIV. Inotropy and cardiac glycoside interaction with cat ventricular muscle. *Mol. Pharmacol.* **16**:135–146

Mitchell, P. 1977. Epilogue: From Energetic abstraction to biochemical mechanism. *Symp. Soc. Gen. Microbiol.* **27**:383–423

Mobley, B.A., Page, E. 1972. The surface area of sheep cardiac Purkinje fibers. *J. Physiol. (London)* **220**:547–563

Mullins, L.J., Frumento, A.S. 1963. The concentration dependence of sodium efflux from muscle. *J. Gen. Physiol.* **46**:629–654

Rapoport, S.I. 1970. The sodium-potassium exchange pump: Relation of metabolism to electrical properties of the cell. I. Theory. *Biophys. J.* **10**:246–259

Sachs, J.R. 1977. Kinetic evaluation of the Na−K pump reaction mechanism. *J. Physiol. (London)* **273**:489–514

Scriven, D.R.L. 1981. Modeling repetitive firing and bursting in a small unmyelinated nerve fiber. *Biophys. J.* **35**:715–730

Skou, J.C. 1957. The influence of some cations on an adenosinetriphosphatase from peripheral nerves. *Biochim. Biophys. Acta* **23**:394–401

Skou, J.C. 1975. The $(Na^+ + K^+)$ activated enzyme system and its relationship to transport of sodium and potassium. *Q. Rev. Biophys.* **7**:401–434

Tanford, C. 1981. Equilibrium state of ATP-driven ion pumps in relation to physiological ion concentration gradients. *J. Gen. Physiol.* **77**:223–229

Veech, R.L., Lawson, J.W.R., Cornell, N.W., Krebs, H.A. 1979. Cytosolic phosphorylation potential. *J. Biol. Chem.* **254**:6538–6547

Received 25 August 1982; revised 3 January 1983